Membrane-Initiated Estrogen Receptor Signaling Mediates Metabolic Homeostasis via Central Activation of Protein Phosphatase 2A

Kazutaka Ueda,[1,2] Eiki Takimoto,[2] Qing Lu,[1] Pangyen Liu,[2] Nobuaki Fukuma,[2] Yusuke Adachi,[2] Ryo Suzuki,[3] Shengpu Chou,[3] Wendy Baur,[1] Mark J. Aronovitz,[1] Andrew S. Greenberg,[4] Issei Komuro,[2] and Richard H. Karas[1]

OBESITY STUDIES

Women gain weight and their diabetes risk increases as they transition through menopause; these changes can be partly reversed by hormone therapy. However, the underlying molecular mechanisms mediating these effects are unknown. A novel knock-in mouse line with the selective blockade of the membrane-initiated estrogen receptor (ER) pathway was used, and we found that the lack of this pathway precipitated excessive weight gain and glucose intolerance independent of food intake and that this was accompanied by impaired adaptive thermogenesis and reduced physical activity. Notably, the central activation of protein phosphatase (PP) 2A improved metabolic disorders induced by the lack of membrane-initiated ER signaling. Furthermore, the antiobesity effect of estrogen replacement in a murine menopause model was abolished by central PP2A inactivation. These findings define a critical role for membrane-initiated ER signaling in metabolic homeostasis via the central action of PP2A.

Obesity is strongly associated with the development of metabolic disorders, including type 2 diabetes, dyslipidemia, and hypertension, as well as an increased risk of cardiovascular diseases (1). Increased prevalence of obesity and associated metabolic disorders in postmenopausal women suggests that the female steroid hormone estrogen mediates metabolic homeostasis (2). Observational studies have shown that certain metabolic conditions, such as obesity and insulin resistance, are strongly related to

estrogen withdrawal (3–6). Ovariectomized rodents consistently exhibit increased body weight and glucose intolerance, which are reversed with estrogen treatment (7,8). However, estrogen replacement as a clinical approach is limited owing to its gynecological and tumor-promoting actions revealed by randomized controlled trials (9). Altogether, these findings underscore the complexity of estrogen's physiological functions, highlight its ability to exert both harmful and beneficial effects, and strongly support the need for better understanding of molecular mechanisms underlying estrogen's effects on metabolism.

Studies using genetically modified mice provide valuable mechanistic insights. Transgenic mice with inactivated aromatase enzyme that is essential for estrogen synthesis exhibit increased adiposity and insulin levels (10). Complete ablation of the estrogen receptor (ER) isoform ERα in mice results in metabolic syndrome-like phenotypes, including increased body weight, adiposity, altered glucose homeostasis, decreased energy expenditure, hyperinsulinemia, and hyperleptinemia (11,12). Meanwhile, contribution of the ER isoform ERβ to metabolic homeostasis is still debatable (13–15).

ERs are ligand-activated transcription factors that, upon binding to specific ligands, form dimers to interact with canonical ER response elements (EREs) in the promotor regions of estrogen-regulated genes. This canonical ER pathway is involved in several estrogen-mediated

[1]Molecular Cardiology Research Institute, Tufts Medical Center, Boston, MA
[2]Department of Cardiovascular Medicine, Graduate School of Medicine, The University of Tokyo, Tokyo, Japan
[3]Department of Diabetes and Metabolic Diseases, Graduate School of Medicine, The University of Tokyo, Tokyo, Japan
[4]Obesity and Metabolism Laboratory, U.S. Department of Agriculture Human Nutrition Research Center on Aging at Tufts University, Boston, MA

Corresponding author: Issei Komuro, komuro-tky@umin.ac.jp, or Richard H. Karas, richard.karas@gmail.com.

adverse effects such as tumorigenesis. In contrast, noncanonical pathways involve ER interplay with other transcriptional mediators that operate in non-ERE regions. Moreover, ERs localized to caveolae, cell membrane microdomains, can signal without nuclear translocation, which is referred to as the rapid nonnuclear ER pathway (16). To determine which of these multiple ER-mediated signaling pathways specifically mediates these effects, we tested the hypothesis that membrane-initiated ERα signaling plays an important role in the biological regulation of metabolic homeostasis.

We have previously reported that the nonnuclear ER pathway activation by estrogen requires ER binding to the scaffolding protein striatin, which is disrupted by a peptide derived from amino acids 176–253 of ERα, resulting in nonnuclear signaling pathway inhibition while sparing the classic genomic signaling pathway (17,18). Moreover, to distinguish the unique role of nonnuclear ERα signaling from those of other signaling pathways, we recently elucidated specific ERα domains critical for binding with striatin and determined that mutations of amino acids 231, 233, and 234 of ERα from KRR to AAA (KRR mutant ERα) disrupted ERα-striatin binding and blocked rapid nonnuclear ERα signaling with no effect on genomic ERα signaling (19).

In the current study, we established the novel KRR knock-in (KRRKI) mouse line, in which endogenous ERα was replaced by KRR mutant ERα in homozygous (KRR$^{ki/ki}$) mice, leading to exclusive disruption of the membrane-initiated ERα signaling in the presence of an intact ERE-mediated genomic ERα signaling pathway. Using this mouse line, we tested the role of membrane-initiated ERα signaling in metabolic homeostasis and its molecular mechanisms.

RESEARCH DESIGN AND METHODS

Animals
The Tufts Medical Center Institutional Animal Care and Use Committee and the University of Tokyo Ethics Committee for Animal Experiments approved all animal procedures. In the current study, C57BL/6 female mice were used unless otherwise indicated. Mice were fed a normal chow diet (4.4% fat, 3.4 kcal/g) or a high-fat diet (32% fat, 5.1 kcal/g; CLEA Japan, Tokyo, Japan). ERα$^{-/-}$ mice were provided by P. Chambon (University of Strasbourg Institute for Advanced Study, Strasbourg, France). Heterozygous males and females were bred to produce wild-type (WT) (ERα$^{+/+}$) and homozygous null ERα$^{-/-}$ offspring. Mice were genotyped by PCR as previously described (20). Littermate WT mice were used as controls. All experiments were performed on mice at 12 weeks of age unless otherwise indicated.

The KRR$^{ki/ki}$ mouse model was generated by GenOway. A targeted strategy was designed to insert three point mutations into exon 8 of the mouse ERα gene to replace amino acids 235K, 237R, and 238R (corresponding with 231K, 233R and 234R of human ERα, respectively) by alanine (Supplementary Fig. 1). The following alanine-specific codons were used to replace native amino acids 235K, 237R, and 238R: GCC, GCT, and GCA. The mutated

ERα gene was expressed under the control of the endogenous ERα promoter. Mutant mouse strains were generated using C57BL/6 embryonic stem cells. Specifically, embryonic stem cells containing the mutated ERα allele were injected into C57BL/6 blastocytes, and pups were genotyped using PCR with primers as follows: forward, 5′-ACATGAGAAATCCCATAAAACTCAGACCAAAC-3′; reverse, 5′-AAAGCCTCTCCCCATCACATGACCT-3′. Expected sizes of the PCR products in the mutant allele were 246 base pairs for WT and 344 base pairs for KRR$^{ki/ki}$ mice, and WT littermates were used as controls.

Glucose and Insulin Tolerance Tests
Mice were fasted for 16 h and 2 h before intraperitoneal (i.p.) injections of 1 g/kg glucose and 0.5 units/kg insulin, respectively. Blood samples were collected from the tail veins at indicated time points after glucose or insulin administration, and blood glucose levels were measured using a blood glucose monitoring system (OneTouch Ultra; Johnson & Johnson).

Measurement of Food Intake and Body Temperature
Food intake was measured daily at specified ages, and average daily food intake was calculated using data from at least 5 consecutive days. For body temperature measurement, WT, ERα$^{-/-}$, and KRR$^{ki/ki}$ mice were housed individually. Mice had free access to water, but food was restricted to avoid the influence of diet-induced thermogenesis. Core body temperature was measured using a rectal temperature probe. Before cold exposure, mice were housed individually at ambient temperature (22°C) for at least 1 h, and basal body temperature was recorded. Mice were then transferred to a cold room (4°C), and body temperature was recorded every hour for a total of 4 h.

Physiological Analyses
Adiposity in mice was examined using computed tomography (CT) (LaTheta; ALOKA) according to the manufacturer's protocol. Scanning was performed at 1-mm intervals from the diaphragm to the floor of the abdominal cavity. VO$_2$ and locomotor activity were measured using an O$_2$/CO$_2$ metabolic measurement system (MK-5000; Muromachi), as previously described (21), and VO$_2$ was normalized to body weight.

Central and Peripheral Administration of Chemicals
Intracerebroventricular injection was performed as previously described (22). Briefly, mice were anesthetized with isoflurane, a small incision was made in the scalp, and an injection was achieved at a point 1 mm lateral and 1 mm caudal to bregma, at a depth of 2 mm. The volume for all intracerebroventricular injections was 1 μL in a 10-μL syringe (Hamilton). The syringe was left in place for 1 min to allow for infusate diffusion. The proper injection site was verified in pilot experiments by administration and localization of Evans Blue dye. Intracerebroventricular administration of okadaic acid (OA, 20 ng; Abcam) and FTY720 (fingolimod, 2.5 μg; Cayman) was performed twice a week (23,24).

Ovariectomies were performed in 10-week-old mice, as described previously (25). For peripheral estrogen treatment, pellets releasing vehicle or 17β-estradiol (E2) (0.25 mg, 60-day release pellets; Innovative Research of America) were implanted 1 week after ovariectomy. The β_3-adrenergic receptor agonist CL316243 (0.5 mg/kg; Tocris) was administered daily via i.p. route (26).

Histology

Fat pads fixed in 10% formalin were embedded in paraffin and sectioned. Specimens were then stained by hematoxylin and eosin, and cell area was measured using National Institutes of Health (NIH) ImageJ software (http://imagej.nih .gov). Sections of adipose tissue samples were immunohistochemically stained by using primary antibodies to UCP1 (Abcam) and Vectastain ABC kit (Vector Laboratories) according to the manufacturers' instructions. Peroxidase activity was visualized with DAB staining (Vector Laboratories), and sections were counterstained with hematoxylin.

Serum Analysis and Protein Phosphatase 2A Activity Assay

Serum estradiol and leptin levels were measured using ELISA (Cayman and Millipore, respectively) according to the manufacturers' protocols. Protein phosphatase (PP) 2A activity was measured using an immunoprecipitation phosphatase assay kit (Merck) according to the manufacturer's instructions. Briefly, tissues were lysed with the IP Lysis Buffer (Thermo Fisher Scientific) supplemented with a protease inhibitor cocktail. Phosphatase inhibitor was not added into the samples. Each sample (400 µg) was immunoprecipitated with a PP2Ac antibody. Beads bound to immunoprecipitated PP2Ac were added to the phosphatase reaction containing a threonine phosphopeptide in a shaking incubator. Samples were then aliquoted into 2 wells of a 96-well plate, and the malachite green detection solution provided by the kit was added. Plates were incubated for 15 min at room temperature, and the absorbance was determined on an automated plate reader. Absorbance was calculated using a standard curve ranging between 0 and 2,000 pmol/L. PP2B activity was measured using a calcineurin activity assay kit (Merck) according to the manufacturer's instructions.

Cell Culture, Transient Transfections, and Luciferase Reporter Assays

Carotid artery smooth muscle cells were cultured from carotid artery explants from KRR[ki/ki] and littermate WT mice and grown in phenol red–free DMEM with 10% charcoal-stripped bovine growth serum (stripped BGS). Cells were cotransfected with an estrogen response element–luciferase reporter plasmid, a β-galactosidase expression plasmid, and ERα expression plasmid. Cells were lysed in the reporter lysis buffer (Promega), and luciferase (Luciferase Assay System; Promega) and β-galactosidase (Tropix) assays were performed according to the manufacturers' guidelines. NIH 3T3-L1 preadipocytes were cultured and differentiated, as previously described (27,28). Briefly, cells were grown in phenol red–free DMEM with 10% calf serum. Two days after reaching confluency, differentiation was initiated with 10% charcoal-stripped FBS (stripped FBS) containing 0.5 mmol/L isobutyl-methylxanthine, 0.25 µmol/L dexamethasone, and 1 µg/mL insulin, and cells were treated with control vehicle, 100 nmol/L E2, or 2 µmol/L rosiglitazone (Sigma-Aldrich). Cells were collected with lysis buffer 72 h later, followed by mRNA extraction.

Coimmunoprecipitation, Immunoblotting, and Phospho-Kinase Array

Tissue proteins were extracted in IP Lysis Buffer (Thermo Fisher Scientific) mixed with cOmplete Protease Inhibitor Cocktail (Roche), and lysates were incubated overnight at 4°C with 5 µg anti-ERα (MC20; Santa Cruz Biotechnology) or anti-striatin (BD Bioscience) antibody. Next, the lysates were incubated with protein G beads (Amersham Biosciences) for 2 h at 4°C, and the pellets obtained after centrifugation were washed five times and analyzed by immunoblotting. Proteins were resolved by dodecyl sulfate-PAGE, transferred to polyvinylidene fluoride membranes, and probed with the appropriate primary antibodies, including AMPK, GAPDH (Santa Cruz Biotechnology), PP2Ac (Millipore), phospho (p)-AMPK, p-Akt, total Akt (Cell Signaling Technology), and α-tubulin (EMD). Membranes were then incubated with the appropriate secondary antibodies and developed using ECL Prime (Amersham Biosciences). The Proteome Profiler Antibody Array (R&D Systems) was used for phospho-kinase analysis, according to the manufacturer's instructions.

Quantitative RT-PCR

Total RNA from adipose tissue samples was extracted using the Lipid RNeasy kit (Qiagen). A total of 1.5 µg RNA from each sample was used to generate cDNA using the SuperScript VILO cDNA Synthesis Kit (Invitrogen). Quantitative (q)RT-PCR was performed on an Eppendorf *realplex*^{2} system using QuantiTect SYBR Green (Qiagen). The specific primers are listed in Supplementary Table 1. Relative expression levels of target genes were calculated using the comparative threshold cycle method. Each sample was run in duplicate, and the results were systematically normalized using *gapdh*. Mitochondrial DNA was amplified using primers *nd1* and *cox1* and normalized to genomic DNA by a primer amplifying *Lpl*.

Statistics

All data are presented as means ± SEM. Comparisons between two groups were performed using the two-tailed Student *t* test, and multiple group comparisons were performed by ANOVA by the Tukey post hoc test. All statistical analyses were performed using GraphPad Prism software (GraphPad Software). *P* values of <0.05 were considered statistically significant.

RESULTS

Loss of Membrane-Initiated ERα Signaling Disrupts Energy and Glucose Homeostasis

First, we confirmed that ERα-striatin binding was disrupted in the uterine tissue of KRR[ki/ki] mice (Fig. 1*A*) and that
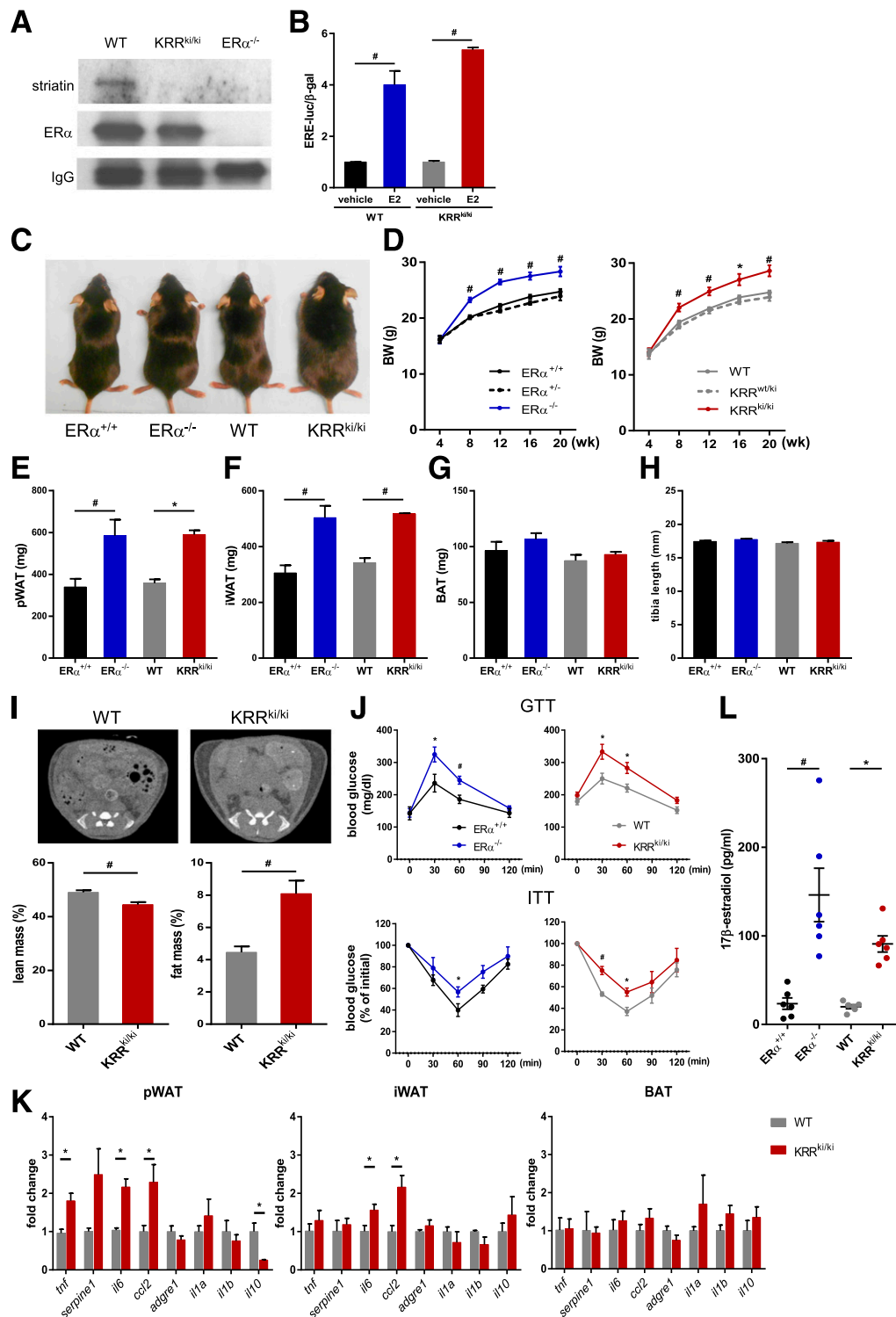
Figure 1—Membrane-initiated signaling is essential for ERα-mediated metabolic homeostasis. *A*: Coimmunoprecipitation of ERα with striatin. Proteins were extracted from uterus tissue of WT, KRR$^{ki/ki}$, and ERα$^{-/-}$ mice, immunoprecipitated using an ERα antibody, and immunoblotted using an antibody against striatin. A representative immunoblot is shown. *B*: Carotid artery VSMCs from WT and KRR$^{ki/ki}$ mice were transiently cotransfected with an estrogen response element–driven luciferase reporter plasmid and a β-galactosidase expression plasmid. Cells were treated with vehicle or E2 for 24 h (*n* = 3). #*P* < 0.01. *C*: Gross appearance of ERα$^{+/+}$, ERα$^{-/-}$, WT, and KRR$^{ki/ki}$ mice. *D*: Body weight (BW) of female mice (*n* = 8–12) over the course of the study. **P* < 0.05, #*P* < 0.01 vs. ERα$^{-/-}$ (left panel) or WT (right panel) mice. *E–H*: Weights of pWAT and iWAT and BAT fat pads as well as the tibia lengths of WT, KRR$^{ki/ki}$, and ERα$^{-/-}$ mice at 12 weeks of age (*n* = 8–12). **P* < 0.05, #*P* < 0.01. *I*: Evaluation of fat and lean mass via CT imaging (*n* = 9–11). #*P* < 0.05. *J*: Glucose tolerance test (GTT) and insulin tolerance test (ITT) results were assessed (*n* = 6–8). **P* < 0.05, #*P* < 0.01. *K*: qRT-PCR analysis for inflammatory cytokines (*n* = 3–6 per group). **P* < 0.05. *L*: Serum E2 levels (*n* = 6 per genotype). **P* < 0.05, #*P* < 0.01. Data are represented as mean ± SEM.

E2 increased transcriptional activity via ERE in carotid artery vascular smooth muscle cells (VSMCs) derived from KRR$^{ki/ki}$ and littermate WT mice (Fig. 1B). Consistently, the disruption of ERα-striatin binding was observed in other organs, such as adipose and brain tissues, and there was no difference in expression levels of ERE-related genes in hypothalamus tissues between the genotypes (Supplementary Fig. 2A and B) (29). On one hand, these data support that the ERα-striatin binding, which is essential for membrane-initiated ER pathway activation, was successfully disrupted in KRR$^{ki/ki}$ mice in various tissues, whereas the ERE-dependent genomic signaling was preserved. On the other hand, ERβ expression levels were comparable between the genotypes, indicating that ERβ signaling was unlikely affected by KI of the mutant ERα (Supplementary Fig. 2C).

Next, we determined the metabolic phenotypes of KRR$^{ki/ki}$ and ERα homozygous-null (ERxα$^{-/-}$) mice. The body weights in female KRR$^{ki/ki}$ mice were significantly higher than those of female WT and heterozygous (KRR$^{wt/ki}$) mice beginning at 2 months of age, which remained higher until the end of the study (Fig. 1C and D). Conversely, the body weights were lower in male KRR$^{ki/ki}$ mice than in male WT mice between 1 and 2 months of age; however, the difference was no longer significant at ≥3 months (Supplementary Fig. 2D). Similar body weight phenotypes were observed in ERα$^{-/-}$ mice (Fig. 1C and D) compared with KRRKI.

The weights of inguinal (subcutaneous) and parametrial (visceral) white adipose tissues (iWAT and pWAT, respectively) were significantly higher in female KRR$^{ki/ki}$ mice than in littermate female WT mice, whereas no difference in interscapular brown adipose tissue (BAT) weights was observed between the two groups (Fig. 1E–G). Comparable tibia lengths between the two genotypes (Fig. 2H) suggest that the increased WAT weight was independent of body growth. Similar changes were observed between the ERα$^{-/-}$ and ERα$^{+/+}$ mice (Fig. 1E–G). Body composition analysis using CT revealed a significant increase in fat mass with a corresponding decrease in lean mass in KRR$^{ki/ki}$ mice compared with that in littermate WT mice (Fig. 1I).

Inflammation plays a critical role in the development of glucose intolerance and insulin resistance, both of which are caused by excessive visceral adipose tissue accumulation (30–32). Previous studies have reported that ERα$^{-/-}$ mice have glucose intolerance accompanied by increased adipose tissue inflammation (33,34). Consistently, KRR$^{ki/ki}$ mice showed impaired glucose tolerance and enhanced insulin resistance at similar levels to those observed in ERα$^{-/-}$ mice (Fig. 1J). Further, mRNA expression levels of inflammatory cytokines, such as tumor necrosis factor (TNF)-α (tnf), plasminogen activator inhibitor (PAI) 1 (serpine1), interleukin (IL) 6 (il6), and monocyte chemoattractant protein (MCP) 1 (ccl2), were higher and that of an anti-inflammatory cytokine IL10 (il10) was lower in KRR$^{ki/ki}$ pWAT than in littermate WT mice iWAT, and increases of IL6 and MCP1 expression were also observed in KRR$^{ki/ki}$ iWAT compared with WT mice; these differences were not observed in BAT (Fig. 1K). These results support that the lack of membrane-initiated ERα signaling induced adipose tissue inflammation, predominantly in WAT, potentially contributing at least in part to impaired glucose homeostasis.

Serum E2 levels were more than four times higher in KRR$^{ki/ki}$ mice than in littermate WT mice (90.9 vs. 20.0 pg/mL, $P < 0.05$); a similar trend was observed between ERα$^{-/-}$ and ERα$^{+/+}$ mice (Fig. 1L). Comparison of body weights of KRR$^{ki/ki}$ mice, with or without ovariectomy, revealed that reduced E2 levels after ovariectomy in KRR$^{ki/ki}$ mice did not affect body weight gain, whereas significant increases in body weight were observed in littermate WT mice (Supplementary Fig. 2E), suggesting that higher E2 levels in KRR$^{ki/ki}$ mice were not associated with increased body weight.

Loss of Membrane-Initiated ERα Signaling Decreases Energy Expenditure Independently of Food Intake

Alterations in food intake or energy expenditure can lead to obesity; however, there was no significant difference in food intake between genotypes (Fig. 2A). Serum leptin levels were significantly upregulated in KRR$^{ki/ki}$ mice consistent with obesity (Fig. 2B), suggesting leptin resistance. VO$_2$ in mice individually housed in metabolic chambers was significantly lower in KRR$^{ki/ki}$ mice than WT mice (Fig. 2C), suggesting that energy expenditure was reduced in KRR$^{ki/ki}$ mice independent of food intake.

Energy expenditure is determined by thermogenesis and physical activity. The core body temperature of KRR$^{ki/ki}$ mice was significantly lower than that of littermate WT mice at ambient temperature (23°C) (Fig. 2D). In addition, acute exposure to cold over 4 h to determine thermogenic function led to significantly lower body temperatures in KRR$^{ki/ki}$ mice than in WT mice (Fig. 2E), despite comparable levels of skeletal muscle shivering between the genotypes. The results from ERα$^{-/-}$ mice were consistent with those from KRR$^{ki/ki}$ mice (Fig. 2A, B, D, and E). Moreover, locomotor activity was significantly lower in KRR$^{ki/ki}$ mice than in WT mice (Fig. 2F). These results suggested that the disruption of membrane-initiated ERα signaling impaired thermogenesis and decreased physical activity.

To exclude the influence of body weight differences between the genotypes, we further examined the energy expenditure earlier at 4 weeks of age when body weight had not significantly diverged (Supplementary Fig. 3A). We observed a significant decrease in body temperature at ambient temperature, VO$_2$, and locomotor activity in KRR$^{ki/ki}$ mice as well, despite no difference observed in food intake (Supplementary Fig. 3B–E).

Lack of Membrane-Initiated ERα Signaling Disrupts Thermogenic Program Accompanied With Depressed β$_3$-Adrenergic Receptor Signaling

Nonshivering thermogenesis is mainly mediated by brown adipocytes in BAT, which generate heat through the mitochondrial uncoupling protein UCP1. Brown adipocyte-like phenotype has been reported in WAT, in a process called "browning" or "beiging," which could mediate
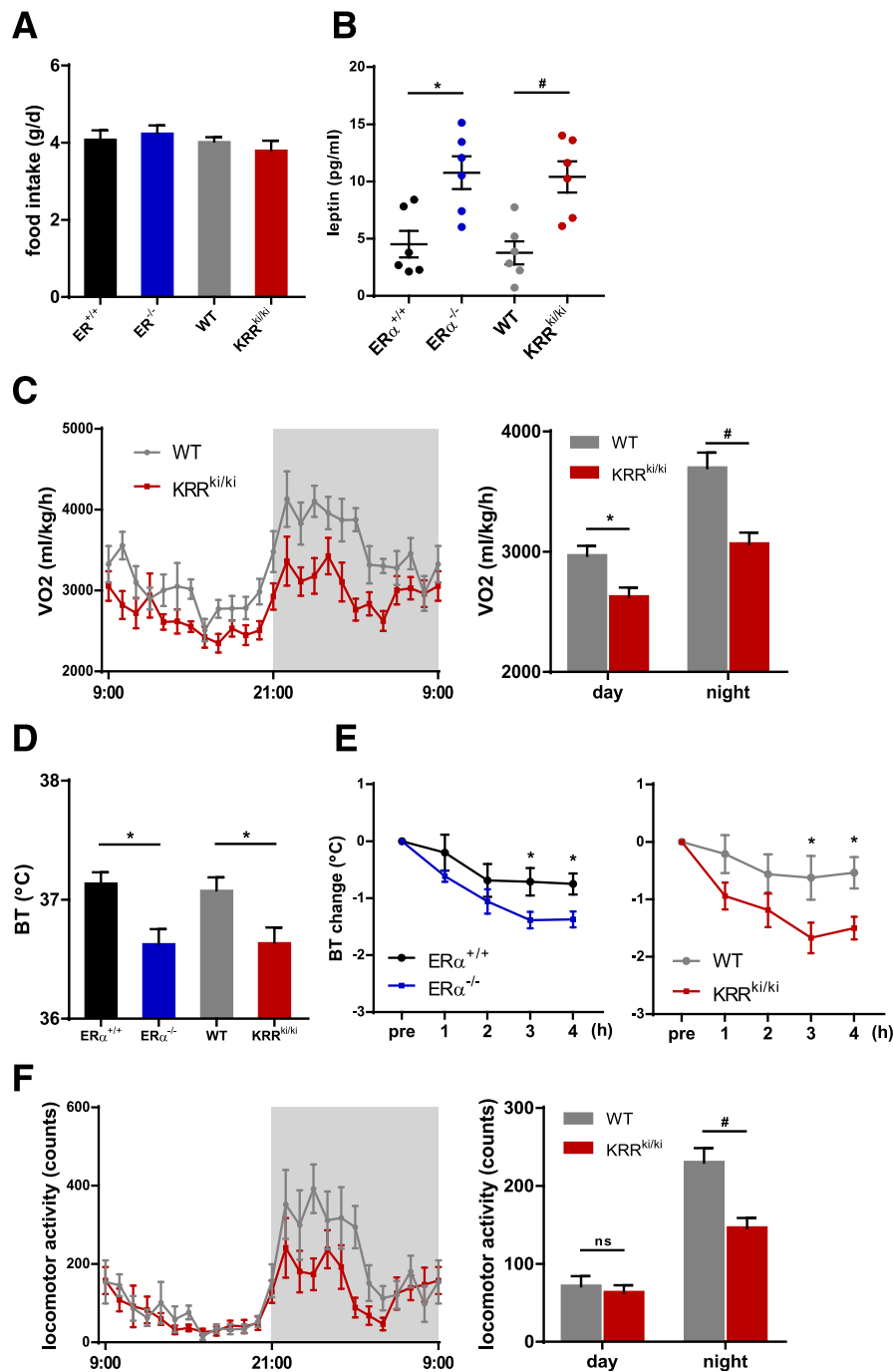
Figure 2—Disruption of membrane-initiated ERα signaling alters energy balance independently of food intake. *A*: Daily food intake ($n = 7$ per group). *B*: Serum leptin concentrations ($n = 6$ per group). *$P < 0.05$, #$P < 0.01$. *C*: Comparison of VO$_2$ in WT and KRR[ki/ki] mice. The data were normalized to body weight. The graph depicts changes in average VO$_2$ during the light (day) and dark (night) phases ($n = 9$ per group). *$P < 0.05$, #$P < 0.01$. *D*: Core body temperature (BT) at ambient atmosphere (22°C) in 12-week-old mice ($n = 8$–10 per group). *$P < 0.05$. *E*: Changes in body temperature of ERα^{+/+}, ERα^{−/−}, WT, and KRR[ki/ki] mice exposed to cold (4°C) for the indicated times ($n = 6$–8 per group). *$P < 0.05$. *F*: Locomotor activity of WT and KRR[ki/ki] mice. The graph depicts changes in average locomotor activity during the light (day) and dark (night) phases ($n = 9$ per group). #$P < 0.01$. Data are represented as mean ± SEM.

thermogenesis and metabolism (35,36). We observed no significant differences in BAT UCP1 protein or mRNA expression levels between WT and KRR[ki/ki] mice (Fig. 3*A* and *B*). In contrast, pWAT UCP1 expression was significantly decreased in KRR[ki/ki] mice (Fig. 3*A* and *B*). Consistently, mRNA

levels of other genes consistent with brown/beige adipocytes, such as *elovl3*, *cidea*, and *cox8b*, were also lower in KRR[ki/ki] pWAT than in WT pWAT (Fig. 3*B*), whereas these changes were not observed in BAT or iWAT (Fig. 3*B*). In addition, in KRR[ki/ki] pWAT, genes associated with mitochondrial
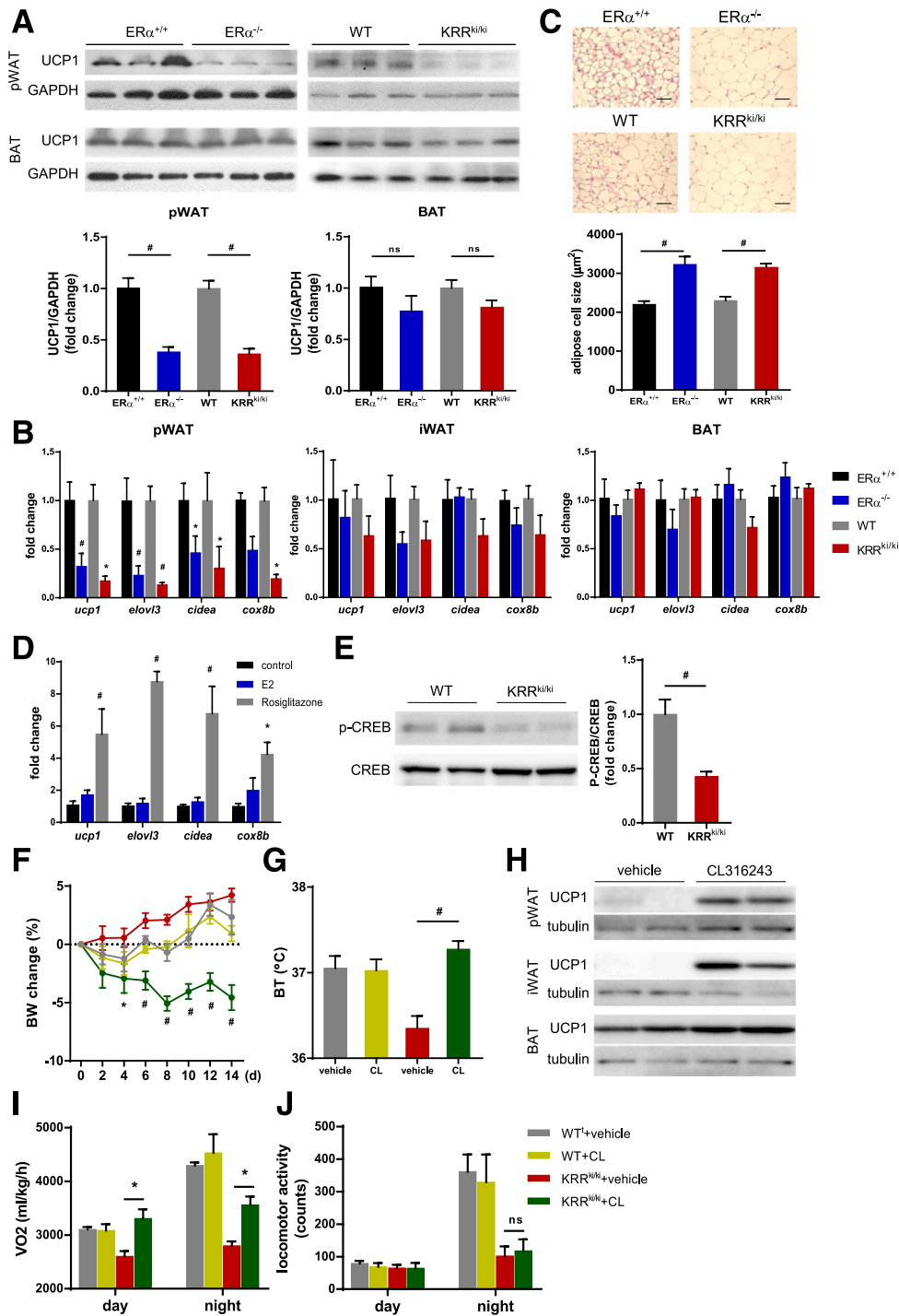
Figure 3—Thermogenic program and β_3-adrenergic receptor signaling is mediated by membrane-initiated ERα signaling. *A*: Immunoblot analysis of UCP1 levels in BAT and pWAT of ER$\alpha^{+/+}$, ER$\alpha^{-/-}$, WT, and KRR$^{ki/ki}$ mice. Representative immunoblots and quantification are shown (*n* = 5–8 per group). #*P* < 0.01. *B*: qRT-PCR analysis of genes consistent with beige adipocytes in adipose tissues of ER$\alpha^{+/+}$, ER$\alpha^{-/-}$, WT, and KRR$^{ki/ki}$ mice (*n* = 6–8). Relative mRNA expression levels are normalized to *gapdh*. **P* < 0.05, #*P* < 0.01. *C*: Hematoxylin and eosin staining of pWAT of ER$\alpha^{+/+}$, ER$\alpha^{-/-}$, WT, and KRR$^{ki/ki}$ mice. Scale bar indicates 100 μm. The graph depicts the quantification of mean cell area (*n* = 4). #*P* < 0.01. *D*: qRT-PCR analysis of genes consistent with beige adipocytes in NIH 3T3-L1 preadipocytes treated with vehicle (control), 100 nmol/L E2, or 2 μmol/L rosiglitazone for 72 h. Relative mRNA expression levels are normalized to *gapdh*. Data depict the results from three independent experiments. **P* < 0.05, #*P* < 0.01. *E*: Immunoblot analysis of p-CREB and total CREB levels in pWAT of WT and KRR$^{ki/ki}$ mice. Representative immunoblots and quantification are shown (*n* = 4). #*P* < 0.01. Changes in body weight (BW) (*F*) and body temperature (BT) (*G*) in WT and KRR$^{ki/ki}$ mice that were i.p. injected daily with vehicle control or 0.5 mg/kg CL316243 (CL) (*n* = 6 for each group). #*P* < 0.01 vs. KRR$^{ki/ki}$ + vehicle. *H*: Representative immunoblot analysis of UCP1 levels in adipose tissues of KRR$^{ki/ki}$ mice treated daily with vehicle control or CL for 14 days. CL treatment led to increased VO$_2$ (*I*) but not locomotor activity (*J*) in KRR$^{ki/ki}$ mice (*n* = 6 per group). **P* < 0.05. Data are represented as mean ± SEM.

biogenesis, including PGC1α (*ppargc1a*) and *nrf1*, were suppressed (Supplementary Fig. 4A), and mitochondrial DNA content indicated by *nd1* and *cox1* expression was also suppressed in KRR[ki/ki] pWAT (Supplementary Fig. 4B). Histological analysis revealed that lipid droplet size was larger and UCP1 expression was decreased in KRR[ki/ki] pWAT compared with WT mice (Fig. 3C and Supplementary Fig. 4C). These changes, which were consistently observed in ERα^{−/−} mice (Fig. 3A–C), suggested that the disruption of membrane-initiated ERα signaling attenuated beiging of adipocytes in female pWAT.

To examine the direct effect of estrogen on gene expression consistent with beiging, we used an established preadipocyte cell line, NIH 3T3-L1. Unexpectedly, E2 had minimal effect on genes, consistent with beige adipocytes in 3T3-L1 cells (Fig. 3D), although rosiglitazone, which promotes beiging (37), significantly increased the expression levels of these genes, suggesting that the direct effects of estrogen signaling on beige adipocyte development were marginal at least in 3T3-L1 preadipocytes.

Adaptive thermogenesis is mainly regulated by sympathetic tone through β-adrenergic signaling. Activated β3-adrenergic receptor by catecholamines in adipocytes phosphorylates several signaling cascades, including protein kinase A and mitogen-activated protein kinases, leading to the phosphorylation of CREB, an important transcription factor that mediates the thermogenic program (38). Levels of p-CREB were lower in KRR[ki/ki] pWAT than in littermate WT mice (Fig. 3E), suggesting attenuated β3-adrenergic receptor signaling in KRR[ki/ki] pWAT. The i.p. administration of the specific β3-adrenergic receptor agonist CL316243 promoted weight loss in KRR[ki/ki] mice accompanied by increased core body temperature (Fig. 3F and G). Furthermore, activation of the β-adrenergic signaling increased UCP1 expression levels in all adipose tissues and VO_2 during daytime (Fig. 3H and I), whereas no significant differences in VO_2 during nighttime or locomotor activity was observed (Fig. 3I and J), suggesting that signal input from sympathetic nerves in the adipose tissue of KRR[ki/ki] mice was attenuated, whereas the response to β3-adrenergic receptor signaling remained intact. These results indicate the existence of sympathetic tone regulation by central action of membrane-initiated ER signaling.

Membrane-Initiated ERα Signaling Regulates Phosphorylation of Multiple Kinases Through PP2A in Hypothalamus

The hypothalamus coordinates the central autonomic network and plays a prominent role in the regulation of energy homeostasis through the control of thermogenesis and physical activity (39,40), where several protein kinases are considered as key players in this regulation (41–43). We therefore examined a role of membrane-initiated ER signaling in activities of kinase signaling in the hypothalamus. Using a phospho-kinase array, we determined that the phosphorylated levels of a subset of kinases, including

AMPK and Akt, were higher in the hypothalamus of KRR[ki/ki] mice than in that of WT mice (Supplementary Fig. 5). Additional immunoblotting using multiple samples showed that these changes were statistically significant (Fig. 4A).

We have previously reported that estrogen activates PP2A in VSMCs via an increase in PP2Ac-striatin complex formation, leading to the inhibition of phosphorylation of several kinases, including Akt, in a rapid nonnuclear signaling–dependent manner (44). Consistently, PP2A activity was significantly lower in the hypothalamus of KRR[ki/ki] mice than in that of littermate WT mice (Fig. 4B), whereas total levels of mRNAs coding for PP2Ac isoforms were similar between the two genotypes (Fig. 4C). Furthermore, coimmunoprecipitation analysis showed that striatin-PP2Ac complex formation was attenuated in the hypothalamus of KRR[ki/ki] mice (Fig. 4D).

Central PP2A Activation Rescues Metabolic Abnormality in KRR[ki/ki] Mice

To investigate the relationship between attenuated PP2A activation in the hypothalamus of KRR[ki/ki] mice and energy balance, we administered a structural analog of sphingosine-1-phosphate and a potent PP2A activator (45,46), FTY720, to KRR[ki/ki] mice via intracerebroventricular injection. FTY720 induced significant weight loss (Fig. 5A) and reversed the metabolic disturbances, such as accumulation of fat mass, lower core body temperature, decreased VO_2 and locomotor activity, and impaired glucose tolerance, observed in KRR[ki/ki] mice (Fig. 5B–F), whereas food intake was not altered (Supplementary Fig. 6A), suggesting that FTY720 rescued the metabolic disorder observed in KRR[ki/ki] mice without nonspecific toxic effects resulting in hypophagia.

Furthermore, PP2A activity was increased, whereas the phosphorylation levels of AMPK and Akt were significantly decreased in the hypothalami of FTY720-treated KRR[ki/ki] mice (Fig. 5G and H); meanwhile, PP2B activity was not altered (Fig. 5G). Consistently, FTY720 increased several genes consistent with beige adipocytes, including UCP1 in pWAT, whereas these changes were not detected in iWAT or BAT (Fig. 5I). In contrast, PP2A activities in adipose tissues were not altered by FTY720 treatment (Supplementary Fig. 6B), suggesting a negligible effect of FTY720 intracerebroventricular injection on peripheral tissues. These data indicate that increased PP2A activity in the hypothalamus restored impaired metabolic homeostasis in KRR[ki/ki] mice.

PP2A Blockade in the Brain Inhibits the Antiobesity Effect of Estrogen

We examined the effects of PP2A inhibition in the central nervous system (CNS) on estrogenic regulation of energy balance in a model of menopause using ovariectomized mice. The body weight gain observed in ovariectomized mice fed the high-fat diet was significantly inhibited with estrogen replacement via implantation of E2-releasing
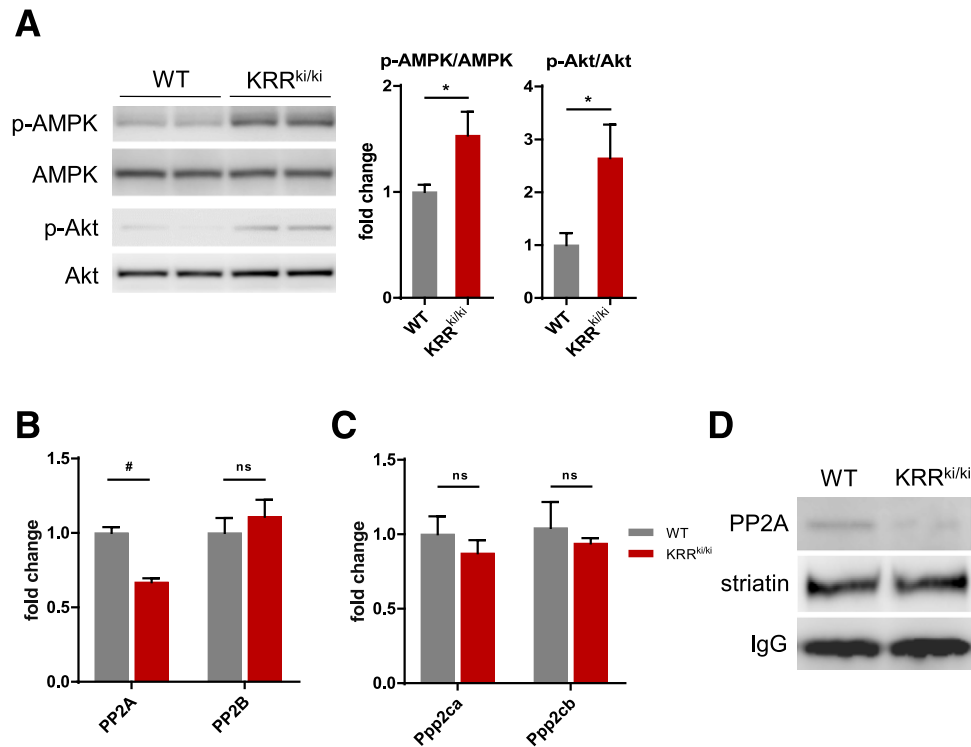
Figure 4—Distinct activation of multiple kinase signaling in hypothalamus of KRR[ki/ki] mice. *A*: Immunoblot analysis of p-AMPK and p-Akt levels in the hypothalami of WT and KRR[ki/ki] mice. A representative immunoblot and quantification are shown (*n* = 4–7 per group). *$P < 0.05$. *B*: PP2A activity in the hypothalami of WT and KRR[ki/ki] mice (*n* = 9 per group). #$P < 0.01$. *C*: qRT-PCR analysis showing no significant differences in the expression levels of PP2Ac coding genes in the hypothalami of WT and KRR[ki/ki] mice (*n* = 4). *D*: Coimmunoprecipitation of striatin with PP2Ac. Striatin was immunoprecipitated from the hypothalami of WT and KRR[ki/ki] mice and immunoblotted for PP2Ac and striatin. Results are representative of three biological replicates. Data are represented as mean ± SEM.

pellets (Fig. 6*A*). Notably, this effect of E2 on weight was abolished by intracerebroventricular administration of a pharmacological PP2A inhibitor, OA (Fig. 6*A*). Consistently, intracerebroventricular OA administration decreased core body temperature, VO₂, locomotor activity, and expression of genes consistent with beige adipocytes (Fig. 6*B*–*D*). These results support that PP2A is a crucial mediator of the antiobesity effect of estrogen in female mice.

DISCUSSION

Sex steroids exert pleiotropic cellular functions. Estrogen has critical roles in the control of not only female fertility but also a wide spectrum of physiological functions, including energy metabolism. Although studies of genetically modified mice have revealed that whole-body ERα deletion in mice causes body weight gain characterized by decreased energy expenditure and increased fat accumulation (12,13), the mechanism by which ERα signaling regulates metabolic homeostasis is unclear.

In the current study, we elucidated that membrane-initiated ERα signaling mediated energy balance through PP2A activation in the CNS, revealing a novel mechanism underlying the estrogen-mediated regulation of metabolic homeostasis (Fig. 6*E*). We observed increased body weight,

fat accumulation, glucose intolerance, and insulin resistance in the novel KRR[ki/ki] mice with deficient membrane-initiated ERα signaling and an intact genomic pathway. This phenotype closely resembled the metabolic changes observed in ERα^{−/−} mice. KRR[ki/ki] mice showed decreased energy expenditure accompanied by lower physical activity and impaired adaptive thermogenesis, which was predominantly characterized by a significant reduction in the beige adipocyte genetic program in pWAT. We also found that the phosphorylation levels of multiple kinases, some of which potentially modulate thermogenesis and physical activity, were increased in the hypothalami of KRR[ki/ki] mice, which were attenuated by the central activation of PP2A that resulted in the restoration of energy balance. In addition, although estrogen replacement inhibited body weight gain in ovariectomized mice in a model of menopause, this effect was abolished by central inhibition of PP2A. Taken together, our results support that membrane-initiated ERα signaling mediates metabolic homeostasis thorough the central regulation of PP2A activation.

The diversity of estrogen's physiological actions in various tissues is partly attributable to multiple ER-mediated signaling pathways. ERα and β mediate the main biological functions of estrogen, and these receptors classically signal by regulating gene transcription. The role of rapid nonnuclear ER
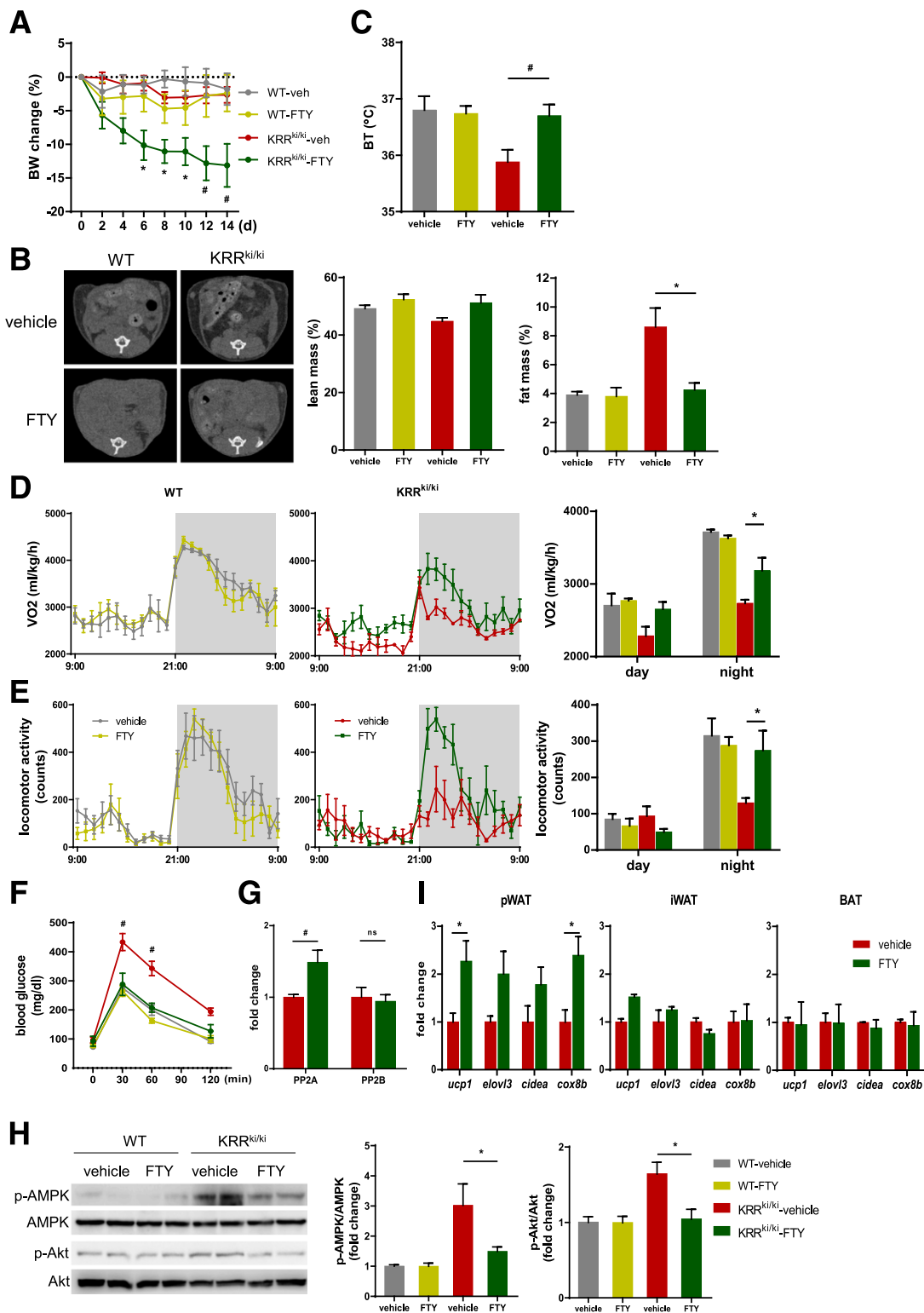
Figure 5—Rescue of central PP2A activity improves metabolic abnormalities in KRR[ki/ki] mice. *A*: Changes in body weight (BW) in WT and KRR[ki/ki] mice that received intracerebroventricular administration of vehicle control (veh) or 2.5 μg FTY720 (FTY) twice a week (*n* = 6 per group). *$P < 0.05$, #$P < 0.01$ vs. KRR[ki/ki] + vehicle. Evaluation of fat and lean mass by CT (*B*), body temperature (BT) (*C*), VO$_2$ (*D*), locomotor activity (*E*), glucose tolerance test (*F*), PP2A and PP2B (calcineurin) activity in hypothalamus (*G*), and qRT-PCR analysis for genes consistent with beige adipocytes (*I*), and representative images of immunoblot analysis for p-AMPK and p-Akt in the hypothalami of WT and KRR[ki/ki] mice treated with intracerebroventricular vehicle control or FTY for 14 days (*H*) (*n* = 5–7 per group). Quantification is shown. *$P < 0.05$, #$P < 0.05$ vs. KRR[ki/ki] + vehicle. Data are represented as mean ± SEM.
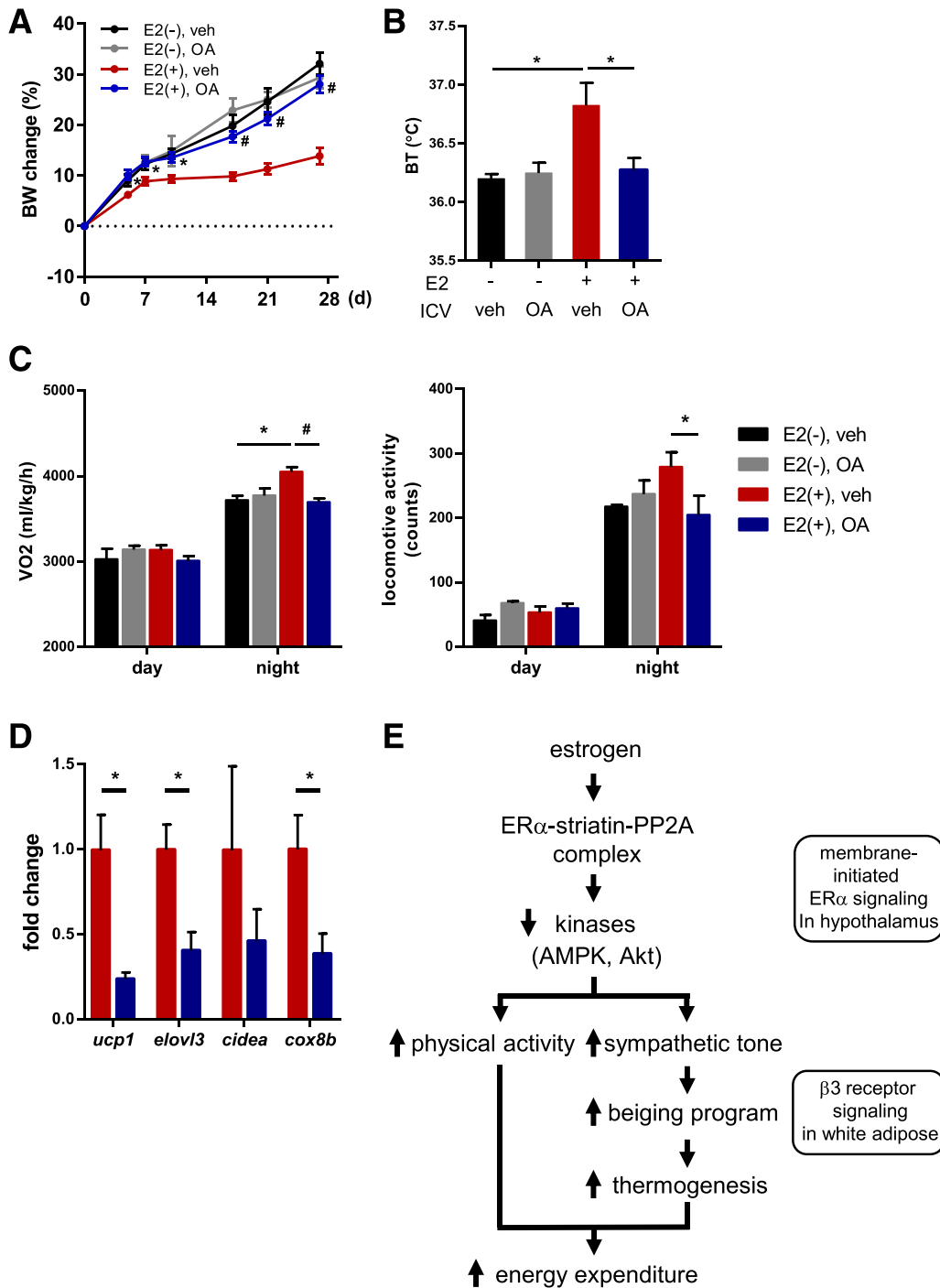
Figure 6—PP2A blockade in the CNS inhibits the antiobesity effect of estrogen. *A*: Changes in body weight (BW) of ovariectomized mice treated with control, E2 pellets, or E2 pellets in combination with 20 ng OA or vehicle control (veh) via intracerebroventricular (ICV) route twice a week (*n* = 7 per group). All mice were ovariectomized and fed a high-fat diet. *$P < 0.05$, #$P < 0.01$ vs. E2 group. Core body temperature (BT) (*B*), VO₂ (left graph) and locomotor activity (right graph) (*C*), and qRT-PCR analysis for genes consistent with beige adipocytes in pWAT (*D*) in mice 14 days after treatment with vehicle (E2) or E2 plus OA. All mice were ovariectomized and implanted with E2 pellets (*n* = 7 per group). *$P < 0.05$, #$P < 0.01$. Data are represented as mean ± SEM. *E*: Proposed mechanisms by which estrogen mediates energy balance through membrane-initiated ER signaling activation in the hypothalamus.

signaling has been implicated in physiological and pathological conditions, including energy homeostasis, but their precise molecular mechanisms have not been elucidated (16). Our findings provide clear evidence that membrane-initiated

ERα signaling is a critical mediator of the effect of estrogen on energy homeostasis. Consistent with this, Park et al. (47) recently demonstrated that the canonical ERE-dependent genomic pathway was not necessary for the effect

of estrogen on energy balance. Moreover, a KI mouse model (NOER mice) in which ERα was replaced with a point mutation of ERα (C451A) that causes the loss of ER palmitoylation, one of the indispensable processes for trafficking of the steroid receptor to the plasma membrane, showed that the loss of membrane ER-mediated signal transduction in response to estrogen was associated with an obesity phenotype (48). This evidence is consistent with our findings implying the importance of the membrane-initiated ERα signaling pathway in energy metabolism.

The hypothalamus is critical for homeostatic regulation, and ERα was shown to be robustly expressed in hypothalamic nuclei, including the ventromedial nucleus, distinct regulators of body weight and glucose homeostasis (49–52). Although some studies showed a significant function for hypothalamic ERα during energy homeostasis in rodents (52), the specific ERα signaling pathway mediating these beneficial functions in the CNS remains unclear. Our observations provide clear evidence that rapid nonnuclear ER signaling mediates the CNS functions of estrogen in a genetically modified mouse model. Intriguingly, recent reports demonstrated that peripheral administration of an estrogen-dendrimer conjugate (EDC) that selectively activated nonnuclear ERα did not prevent the increase in adiposity or glucose intolerance (53,54), implying the possibility that systemically delivered EDC might have limited CNS access due to the blood-brain barrier (54). Central EDC administration might facilitate the understanding of the role of nonnuclear ERα signaling in hypothalamic regulation of energy homeostasis.

PP2A is a major serine/threonine PP that is highly conserved in all eukaryotes and regulates the activity of more than 30 different kinases, including Akt and AMPK, that contribute to the development of obesity (41,55,56). Here we explored the role of PP2A activation in E2-mediated energy expenditure and found that striatin-PP2Ac binding in the hypothalamus was diminished in KRR[ki/ki] mice, resulting in decreased PP2A activity, suggesting that the interaction between ERα, striatin, and PP2Ac and the activity of PP2A was dependent on the rapid nonnuclear ERα pathway. Notably, pharmacological PP2A activation in the CNS by intracerebroventricular administration of FTY720 in KRR[ki/ki] mice led to significant body weight loss accompanied by dephosphorylation of kinases, including AMPK and Akt, in the hypothalamus. These observations indicate the possibility that PP2A activators might act as potential therapeutics against obesity and obesity-associated metabolic disorders, although further investigation is required.

WAT stores energy in the form of triglycerides, whereas BAT and beige adipocytes dissipate energy through uncoupled respiration and heat production (57). Elucidation of BAT-like characteristics in WAT might provide an alternative strategy to increase energy expenditure and prevent weight gain (35). In the current study, we observed significant reductions of UCP1 and other markers of beige adipocytes in pWAT of KRR[ki/ki] mice. Of note, a previous study demonstrated that activation of the β₃-adrenergic receptor in pWAT of female but not male mice increased UCP1 expression (58). These results suggest that that membrane-initiated ERα signaling is a crucial mediator of beiging, especially in female mice.

Prior work has identified some physiological effects of nonnuclear signaling, including our prior work on vascular injury (18). The current work possibly adds the regulation of metabolic homeostasis to this growing list of physiologically important effects of estrogen that are mediated by nonnuclear signaling.

The current study also has limitations. ERα is known to be translocated into the nucleus to regulate gene transcription via other transcription factors that do not bind to ERE (16). Also, a recent study reported that deletion of the activation function domain-2 of ERα inhibits estrogen effects on genomic function and causes obesity (59). Because ERα nonnuclear signaling reportedly affects the ER-mediated genomic function (60), we cannot exclude the possibility that the block of the membrane-initiated ERα signaling in our model caused obesity through ER genomic signaling modulation, independently from the ERE-regulated gene regulation. A previous study using ERα$^{-/-}$ mice showed that the obesity phenotype was observed not only in females but also in males (11), whereas we observed no body weight difference in ERα$^{-/-}$ male mice. This discrepancy might be explained by the time duration of the experiments. In our study, the measurement of the body weight of both KRRKI and ERα$^{-/-}$ mice ended at 20 weeks (140 days of age) but continued for more than 300 days in the prior study. It is possible that the difference in body weight between WT and ERα$^{-/-}$ mice became apparent only after 20 weeks. In addition, CL316243 (0.5 mg/kg) administration induced body weight loss in KRR[ki/ki] mice but not in WT mice (Fig. 3F). Meanwhile, a higher dose CL316243 (1.0 mg/kg) induced body weight loss in both genotypes (data not shown), suggesting higher sensitivity of KRR[ki/ki] mice to activation of the β₃-adrenergic receptor signaling than that of WT mice. We could not clarify in the current study the reason for the different responsiveness between the genotypes. Finally, future studies are needed to evaluate the extent to which our findings in mice translate to humans and to better understand whether there are also unintended effects of PP2A activation in brain.

In conclusion, our results support that membrane-initiated ERα signaling mediated energy balance through PP2A activation in the CNS, whereas its loss led to decreased energy expenditure accompanied by impaired adaptive thermogenesis, which was predominantly characterized by a significant attenuation of the BAT-like gene program in WAT and lower physical activity. We also found that after the loss of membrane-initiated ERα signaling, two kinases, AMPK and Akt, both of which mediate the thermogenic program and physical activity, were differentially regulated in the hypothalamus where PP2A played a crucial role. Taken together, these findings provide novel

mechanistic insights into the relationship between estrogen signaling and metabolism and a novel strategy to attack obesity and subsequent metabolic disorders threatening the well-being of postmenopausal women.

References

1. Wang YC, McPherson K, Marsh T, Gortmaker SL, Brown M. Health and economic burden of the projected obesity trends in the USA and the UK. Lancet 2011;378:815–825

2. Steinbaum SR. The metabolic syndrome: an emerging health epidemic in women. Prog Cardiovasc Dis 2004;46:321–336

3. Nilsson M, Dahlman I, Rydén M, et al. Oestrogen receptor α gene expression levels are reduced in obese compared to normal weight females. Int J Obes 2007; 31:900–907

4. Key TJ, Appleby PN, Reeves GK, et al.; Endogenous Hormones Breast Cancer Collaborative Group. Body mass index, serum sex hormones, and breast cancer risk in postmenopausal women. J Natl Cancer Inst 2003;95:1218–1226

5. Panotopoulos G, Raison J, Ruiz JC, Guy-Grand B, Basdevant A. Weight gain at the time of menopause. Hum Reprod 1997;12(Suppl. 1):126–133

6. Margolis KL, Bonds DE, Rodabough RJ, et al.; Women's Health Initiative Investigators. Effect of oestrogen plus progestin on the incidence of diabetes in postmenopausal women: results from the Women's Health Initiative Hormone Trial. Diabetologia 2004;47:1175–1187

7. Rogers NH, Perfield JW 2nd, Strissel KJ, Obin MS, Greenberg AS. Reduced energy expenditure and increased inflammation are early events in the development of ovariectomy-induced obesity. Endocrinology 2009;150:2161–2168

8. Wohlers LM, Spangenburg EE. 17β-estradiol supplementation attenuates ovariectomy-induced increases in ATGL signaling and reduced perilipin expression in visceral adipose tissue. J Cell Biochem 2010;110:420–427

9. Manson JE, Hsia J, Johnson KC, et al.; Women's Health Initiative Investigators. Estrogen plus progestin and the risk of coronary heart disease. N Engl J Med 2003;349:523–534

10. Jones ME, Thorburn AW, Britt KL, et al. Aromatase-deficient (ArKO) mice have a phenotype of increased adiposity. Proc Natl Acad Sci U S A 2000;97: 12735–12740

11. Heine PA, Taylor JA, Iwamoto GA, Lubahn DB, Cooke PS. Increased adipose tissue in male and female estrogen receptor-α knockout mice. Proc Natl Acad Sci U S A 2000;97:12729–12734

12. Vidal O, Lindberg M, Sävendahl L, et al. Disproportional body growth in female estrogen receptor-α-inactivated mice. Biochem Biophys Res Commun 1999;265:569–571

13. Bryzgalova G, Gao H, Ahren B, et al. Evidence that oestrogen receptor-α plays an important role in the regulation of glucose homeostasis in mice: insulin sensitivity in the liver. Diabetologia 2006;49:588–597

14. Ponnusamy S, Tran QT, Harvey I, et al. Pharmacologic activation of estrogen receptor β increases mitochondrial function, energy expenditure, and brown adipose tissue. FASEB J 2017;31:266–281

15. Miao YF, Su W, Dai YB, et al. An ERβ agonist induces browning of subcutaneous abdominal fat pad in obese female mice. Sci Rep 2016;6: 38579

16. Mendelsohn ME, Karas RH. Rapid progress for non-nuclear estrogen receptor signaling. J Clin Invest 2010;120:2277–2279

17. Lu Q, Pallas DC, Surks HK, Baur WE, Mendelsohn ME, Karas RH. Striatin assembles a membrane signaling complex necessary for rapid, nongenomic activation of endothelial NO synthase by estrogen receptor alpha. Proc Natl Acad Sci U S A 2004;101:17126–17131

18. Bernelot Moens SJ, Schnitzler GR, Nickerson M, et al. Rapid estrogen receptor signaling is essential for the protective effects of estrogen against vascular injury. Circulation 2012;126:1993–2004

19. Lu Q, Schnitzler GR, Ueda K, et al. ER alpha rapid signaling is required for estrogen induced proliferation and migration of vascular endothelial cells. PLoS One 2016;11:e0152807

20. Dupont S, Krust A, Gansmuller A, Dierich A, Chambon P, Mark M. Effect of single and compound knockouts of estrogen receptors alpha (ERalpha) and beta (ERbeta) on mouse reproductive phenotypes. Development 2000;127: 4277–4291

21. Oike Y, Akao M, Yasunaga K, et al. Angiopoietin-related growth factor antagonizes obesity and insulin resistance. Nat Med 2005;11:400–408

22. Haley TJ, McCormick WG. Pharmacological effects produced by intracerebral injection of drugs in the conscious mouse. Br J Pharmacol Chemother 1957;12: 12–15

23. Kamat PK, Tota S, Saxena G, Shukla R, Nath C. Okadaic acid (ICV) induced memory impairment in rats: a suitable experimental model to test anti-dementia activity. Brain Res 2010;1309:66–74

24. Neviani P, Santhanam R, Oaks JJ, et al. FTY720, a new alternative for treating blast crisis chronic myelogenous leukemia and Philadelphia chromosome-positive acute lymphocytic leukemia. J Clin Invest 2007;117:2408–2421

25. Pare G, Krust A, Karas RH, et al. Estrogen receptor-alpha mediates the protective effects of estrogen against vascular injury. Circ Res 2002;90:1087–1092

26. Kim H, Pennisi PA, Gavrilova O, et al. Effect of adipocyte beta3-adrenergic receptor activation on the type 2 diabetic MKR mice. Am J Physiol Endocrinol Metab 2006;290:E1227–E1236

27. Zebisch K, Voigt V, Wabitsch M, Brandsch M. Protocol for effective differentiation of 3T3-L1 cells to adipocytes. Anal Biochem 2012;425:88–90

28. Murase Y, Kobayashi J, Nohara A, et al. Raloxifene promotes adipocyte differentiation of 3T3-L1 cells. Eur J Pharmacol 2006;538:1–4

29. Bourdeau V, Deschênes J, Métivier R, et al. Genome-wide identification of high-affinity estrogen response elements in human and mouse. Mol Endocrinol 2004;18:1411–1427

30. Fox CS, Massaro JM, Hoffmann U, et al. Abdominal visceral and subcutaneous adipose tissue compartments: association with metabolic risk factors in the Framingham Heart Study. Circulation 2007;116:39–48

31. Hotamisligil GS. Inflammation and metabolic disorders. Nature 2006;444: 860–867

32. Lumeng CN, Saltiel AR. Inflammatory links between obesity and metabolic disease. J Clin Invest 2011;121:2111–2117

33. Ribas V, Nguyen MT, Henstridge DC, et al. Impaired oxidative metabolism and inflammation are associated with insulin resistance in ERalpha-deficient mice. Am J Physiol Endocrinol Metab 2010;298:E304–E319

34.   Davis KE, D Neinast M, Sun K, et al. The sexually dimorphic role of adipose and adipocyte estrogen receptors in modulating adipose tissue expansion, inflammation, and fibrosis. Mol Metab 2013;2:227–242

35.   Cypess AM, Lehman S, Williams G, et al. Identification and importance of brown adipose tissue in adult humans. N Engl J Med 2009;360:1509–1517

36.   Seale P, Conroe HM, Estall J, et al. Prdm16 determines the thermogenic program of subcutaneous white adipose tissue in mice. J Clin Invest 2011;121:96–105

37.   Ohno H, Shinoda K, Spiegelman BM, Kajimura S. PPARγ agonists induce a white-to-brown fat conversion through stabilization of PRDM16 protein. Cell Metab 2012;15:395–404

38.   Whittle AJ, Carobbio S, Martins L, et al. BMP8B increases brown adipose tissue thermogenesis through both central and peripheral actions. Cell 2012;149:871–885

39.   Majdic G, Young M, Gomez-Sanchez E, et al. Knockout mice lacking steroidogenic factor 1 are a novel genetic model of hypothalamic obesity. Endocrinology 2002;143:607–614

40.   Kooijman S, van den Heuvel JK, Rensen PC. Neuronal control of brown fat activity. Trends Endocrinol Metab 2015;26:657–668

41.   Klöckener T, Hess S, Belgardt BF, et al. High-fat feeding promotes obesity via insulin receptor/PI3K-dependent inhibition of SF-1 VMH neurons. Nat Neurosci 2011;14:911–918

42.   Kim MS, Pak YK, Jang PG, et al. Role of hypothalamic Foxo1 in the regulation of food intake and energy homeostasis. Nat Neurosci 2006;9:901–906

43.   Martínez de Morentin PB, González-García I, Martins L, et al. Estradiol regulates brown adipose tissue thermogenesis via hypothalamic AMPK. Cell Metab 2014;20:41–53

44.   Ueda K, Lu Q, Baur W, Aronovitz MJ, Karas RH. Rapid estrogen receptor signaling mediates estrogen-induced inhibition of vascular smooth muscle cell proliferation. Arterioscler Thromb Vasc Biol 2013;33:1837–1843

45.   Pippa R, Dominguez A, Christensen DJ, et al. Effect of FTY720 on the SET-PP2A complex in acute myeloid leukemia; SET binding drugs have antagonistic activity. Leukemia 2014;28:1915–1918

46.   Oaks JJ, Santhanam R, Walker CJ, et al. Antagonistic activities of the immunomodulator and PP2A-activating drug FTY720 (Fingolimod, Gilenya) in Jak2-driven hematologic malignancies. Blood 2013;122:1923–1934

47.   Park CJ, Zhao Z, Glidewell-Kenney C, et al. Genetic rescue of nonclassical ERα signaling normalizes energy balance in obese Erα-null mutant mice. J Clin Invest 2011;121:604–612

48.   Pedram A, Razandi M, Blumberg B, Levin ER. Membrane and nuclear estrogen receptor α collaborate to suppress adipogenesis but not triglyceride content. FASEB J 2016;30:230–240

49.   Labbé SM, Caron A, Lanfray D, Monge-Rofarello B, Bartness TJ, Richard D. Hypothalamic control of brown adipose tissue thermogenesis. Front Syst Neurosci 2015;9:150

50.   Xu P, Cao X, He Y, et al. Estrogen receptor-α in medial amygdala neurons regulates body weight. J Clin Invest 2015;125:2861–2876

51.   Musatov S, Chen W, Pfaff DW, et al. Silencing of estrogen receptor alpha in the ventromedial nucleus of hypothalamus leads to metabolic syndrome. Proc Natl Acad Sci U S A 2007;104:2501–2506

52.   Xu Y, Nedungadi TP, Zhu L, et al. Distinct hypothalamic neurons mediate estrogenic effects on energy homeostasis and reproduction. Cell Metab 2011;14:453–465

53.   Chambliss KL, Wu Q, Oltmann S, et al. Non-nuclear estrogen receptor alpha signaling promotes cardiovascular protection but not uterine or breast cancer growth in mice. J Clin Invest 2010;120:2319–2330

54.   Chambliss KL, Barrera J, Umetani M, et al. Nonnuclear estrogen receptor activation improves hepatic steatosis in female mice. Endocrinology 2016;157:3731–3741

55.   Plum L, Ma X, Hampel B, et al. Enhanced PIP3 signaling in POMC neurons causes KATP channel activation and leads to diet-sensitive obesity. J Clin Invest 2006;116:1886–1901

56.   Millward TA, Zolnierowicz S, Hemmings BA. Regulation of protein kinase cascades by protein phosphatase 2A. Trends Biochem Sci 1999;24:186–191

57.   Kajimura S, Seale P, Spiegelman BM. Transcriptional control of brown fat development. Cell Metab 2010;11:257–262

58.   Kim SN, Jung YS, Kwon HJ, Seong JK, Granneman JG, Lee YH. Sex differences in sympathetic innervation and browning of white adipose tissue of mice. Biol Sex Differ 2016;7:67

59.   Handgraaf S, Riant E, Fabre A, et al. Prevention of obesity and insulin resistance by estrogens requires ERα activation function-2 (ERαAF-2), whereas ERαAF-1 is dispensable. Diabetes 2013;62:4098–4108

60.   Prossnitz ER, Barton M. The G-protein-coupled estrogen receptor GPER in health and disease. Nat Rev Endocrinol 2011;7:715–726